Achievable Rate of Indoor THz Communication Systems with Finite-Bit ADCs

Dan Li*, Deli Qiao*, and Lei Zhang†
*School of Information Science and Technology, East China Normal University, Shanghai, China
†School of Engineering, University of Glasgow, Glasgow, U.K.
Email: 51161214012@stu.ecnu.edu.cn, dlqiao@ce.ecnu.edu.cn, lei.zhang@glasgow.ac.uk.

***Abstract*—In this paper, the achievable rate of the downlink terahertz (THz) communication systems equipped with finite-bit analog-to-digital converters (ADCs) at user sides is investigated. Considering the array of subarray anteanna structure, the hybrid precoding with the maximum ratio transmission (MRT) and zero-forcing (ZF) precoding are applied at the baseband. The closed-form expression of the lower bound of the achievable rate is derived when the number of subarray antennas goes to infinity. It is shown that the coarse quantization distortion cannot be ignored in large antenna subarray regime. On the other hand, the rate loss caused by the phase uncertainties can be negligible in large subarray antenna regime. Overall, the impact of quantized receivers on the performance of indoor THz communication systems is characterized.**

I. INTRODUCTION

For future wireless systems with data rates of more than 1 Terabit-per-second (Tbps) [1], terahertz (THz) has been proposed as one of the promising solutions to enable ultra-high-speed communications [2]-[4]. With the available bandwidth being more than one order of magnitude over the micro-/millimeter-wave systems and graphene technology, its application scenario can be ranging from cordless phones with 360° autosterescopic displays, optic-fiber replacement, and wireless Tb/s file transferring [1].

Different from the traditional micro-/millimeter-wave communication, the transmissions in the THz band will experience high molecular absorption and propagation loss. As a result, more antennas are required in the systems to form a high directional beam to counteract the loss. The THz communications have attracted much interest recently [5]-[11]. For instance, the performance of multi-user systems with partial channel state information has been characterized in [9]. The indoor THz communications with antenna subarrays for single users with perfect channel state information have been analyzed in [10]. According to the analysis in [11], hybrid precoding with an array-of-subarrays architecture can improve both the spectral and energy efficiency in the THz communications.

Meanwhile, large number of antennas with high-resolution analog-to-digital converters (ADCs) are high cost and power-inefficient. As a solution to overcome such constraint, the low-resolution converters have been introduced to reduce the hardware cost and power consumption and the analysis of the micro-/millimeter-wave communication systems with low-resolution converters have attracted much interest (see, e.g., [12]-[16] and references therein). For instance, the impact of low-resolution ADCs on the uplink massive MIMO communication system has been discussed in [13], which showed that reliable communications can be achieved and the resolution of ADCs only up to 3 bits can achieve near infinite-resolution performance. The joint effect of finite-bit ADCs at user sides and low-resolution digital-analog converters (DACs) at the base station has been studied in [14], [15], which showed that finite-bit ADCs cause more rate loss than DACs with the same resolution. A capacity lower bound for wideband channels and one-bit ADCs has been derived in [16].

In this paper, we investigate the downlink THz communication system with finite-bit ADCs at user sides while infinity-resolution DACs are assumed at the Access Point (AP). The structure of array-of subarray and hybrid beamforming are assumed at the AP. Before the analog beamforming, we have user-grouping to eliminate the interference among groups and the users in the same group are allocated orthogonal frequencies according to the scheme of distance-aware multi-carrier transmission [8]. Sequentially, in large subarray antenna regime, we derive the closed-form expression of the lower-bound of the achievable rate and investigate the impact of phase errors.

The rest of this paper is organized as follows. Section II presents the system model and preliminaries on indoor THz channel model and the hybrid beamforming scheme. The analyzes of quantized transmission rate in large subarray antenna regime are presented in Section III. Numerical results are given in Section IV. Finally, Section V concludes this paper.

Notation: $\mathbf{C}^T$, $\mathbf{C}^H$, and $tr(\mathbf{C})$ denote the transpose, Hermitian and trace of matrix $\mathbf{C}$, respectively. $\mathrm{diag}(\mathbf{C})$ denotes the main diagonal of the matrix $\mathbf{C}$. $\|\mathbf{C}\|$ is the Frobenius norm of $\mathbf{C}$. $[\mathbf{C}]_{\iota,\ell}$ represents the entry on the ι-th row and the ℓ-th column. $\mathbb{E}[\cdot]$ is the expectation.

II. SYSTEM MODEL AND PRELIMINARIES

In this section, we will first briefly discuss the system model, and then the indoor THz channel model and hybrid precoding scheme, so that the receivers with low-resolution ADCs are considered and the achievable rate is introduced.

A. System Model

We consider the downlink THz communication system with finite-bit ADCs at the receiver while infinity-resolution DACs

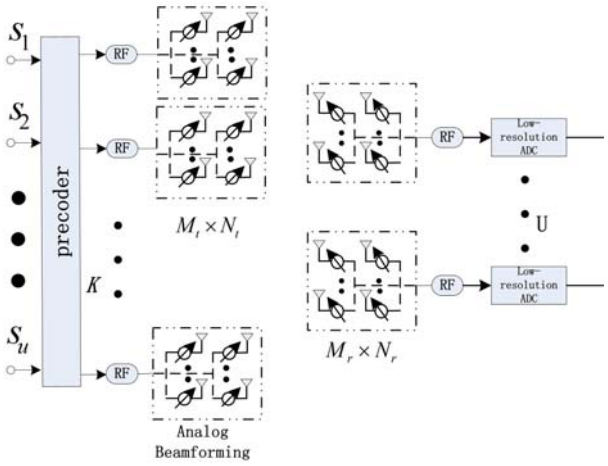

Fig. 1. System model.

are equipped at the transmitter as depicted in Fig.1. In the system, the AP is equipped with K antenna subarrays and each is composed of $M_t \times N_t$ tightly-packed antenna elements. Specifically, each subarray is connected to one radio frequency (RF) chain and each antenna element is driven by an analog phase shifter. Such a design, which is assumed the same as in [11], can reduce the system complexity and improve both the spectral and energy efficiency. At user sides, there is only one subarray of size $M_r \times N_r$ per user. In particular, each subarray is connected to one RF chain with finite-bit ADC.

Denote a as the subarray antenna element spacing. Usually, a is assumed to be less than the wavelength while the spacing between the adjacent subarrays is much larger than the wavelength [11]. In this way, independent channels can be expected for different subarrays. Additionally, the distance from any user to the AP is assumed to be much larger than the spacing between the subarrays, such that the distance between user u and any subarray of the AP is almost the same and denoted as d_u. Besides, K is assumed to be equal to or greater than U to offer sufficient degrees of freedom to all users.

In the THz communication system, the propagation will be affected by the molecular absorption severely in different frequencies. Then, different transmission windows, each with different bandwidth varying with the communication distance, are created and incorporated as an important feature in designing the transmission strategies in the THz band [8]. For example, distance-aware multi-carrier transmission has been proposed and analyzed for indoor THz communications, where the transmission windows, 0.6-0.7 THz and 0.8-0.95 THz, will be assigned to the user with 10 m distance to the AP, while the transmission windows, 0.5-0.6 THz, 0.7-0.8 THz, and 0.95-1 THz, will be allocated to the user 1 m away. Besides, to make full use of the resource, we will allocate the subarrays after user-grouping, and as a result it is obvious that there are different number of users and antenna subarrays in a certain sub-carrier w.

B. Indoor Terahertz Channel Model

The indoor THz channel response for one antenna subarray is given by [10]

$$\begin{aligned}&\mathbf{H}_{sub}(f,d)\\ &=\sqrt{M_tN_tM_rN_r}\big[\eta_L(f,d)\Omega_t\Omega_r\mathbf{a}_r(\psi_L^r,\phi_L^r)\mathbf{a}_t^H(\psi_L^t,\phi_L^t)\\ &+\sum_{i=1}^{J}\eta_i(f,d)\Omega_t\Omega_r\mathbf{a}_r(\psi_i^r,\phi_i^r)\mathbf{a}_t^H(\psi_i^t,\phi_i^t)\big],\end{aligned} \tag{1}$$

where J is the number of non-line-of-sight (NLoS) rays, $\eta(f,d)=|\eta(f,d)|e^{j\vartheta}$ denotes the channel coefficient of the ray with ϑ representing the independent phase shift of each path, and ψ^t/ϕ^t and ψ^r/ϕ^r are the corresponding azimuth and elevation angles of departure and arrival (AoD/AoA) for the rays, respectively. Ω_t and Ω_r are the transmit and receive antenna gains. $\mathbf{a}_r(\psi^r,\phi^r)$ and $\mathbf{a}_t(\psi^t,\phi^t)$ are the subarray steering vectors at the transmit and receive sides, respectively. For an (M,N)-element uniform planar array, the array steering vector is given by

$$\begin{aligned}\mathbf{a}(\psi,\phi)=\frac{1}{\sqrt{MN}}[1,\cdots,e^{j\frac{2\pi a}{\lambda}[m\cos\psi\sin\phi+n\sin\psi\sin\phi]},\\ \cdots,e^{j\frac{2\pi a}{\lambda}[(M-1)\cos\psi\sin\phi+(N-1)\sin\psi\sin\phi]}]^T,\end{aligned} \tag{2}$$

where m and n are the antenna element indexes with $0\le m\le M-1, 0\le n\le N-1$, λ is the wavelength and a is the antenna element spacing.

The THz signals are sensitive to the atmospheric attenuation and molecular absorption. The path gain of the line-of-sight (LoS) path is given by [5]

$$|\eta_L(f,d)|^2=\mathfrak{L}_{asp}(f,d)=\left(\frac{c}{4\pi fd}\right)^2 e^{-\kappa_{abs}(f)d}. \tag{3}$$

where c is the speed of light in free space, f is the carrier frequency, d is the path length, and κ_{abs} is the frequency-dependent medium absorption coefficient, which is decided by the transmission medium at a molecular level. On the other hand, due to the sub-millimeter wavelength of the THz signals, the indoor surfaces are rough at THz frequency, which will introduce additional loss of the NLoS rays [6]. Then, the path gain of the i-th NLoS ray with one reflection is given by

$$|\eta_i(f,d)|^2=\Gamma_i^2(f)\mathfrak{L}_{asp}(f,d), \tag{4}$$

where Γ is the reflection coefficient composed of the Fresnel reflection coefficient and the Rayleigh roughness factor. Note that only up to two reflections are considered in the THz band due to the high reflection losses [6], and the associated path gain can be written similarly to (4). Therefore, the THz channel has limited number of paths.

C. Hybrid Beamforming and Distance-aware Transmission Rate

Based on the structure of antenna subarray, the hybrid beamforming is considered, including the digital beamforming at baseband and analog beamforming at each antenna subarray.

1) Analog Beamforming: Firstly, subarrays activate a set of antennas to produce a beam pre-scanning with an angular separation φ, and the different users in the same angle section are viewed as one group. Denote the user set in group q as $\mathcal{U}_q$. The users in the same group share the set of antenna subarrays $\mathcal{K}_q$. Let (ψ_0^t, ϕ_0^t) be the transmit analog beamforming angle of the subarray $k \in \mathcal{K}_q$. Suppose that (ψ_0^r, ϕ_0^r) is the receive analog beamforming angle of user $u \in \mathcal{U}_q$. Then, the effective channel between the user and the k-th subarray of the AP is given by

$$h_k(f_u^w, d_u) = \mathbf{a}_r^H(\psi_0^r, \phi_0^r)\mathbf{H}_{sub_k}(f_u^w, d_u)\mathbf{a}_t(\psi_0^t, \phi_0^t), \quad (5)$$

where d_u is the distance from the AP to user u.

The transmit beamforming angles for the users in group q, $(\tilde{\psi}_q^t, \tilde{\phi}_q^t)$, and receive beamforming angles for user u in group q, $(\tilde{\psi}_{u,q}^r, \tilde{\phi}_{u,q}^r)$, can be selected from the codebook as follows

$$\{(\tilde{\psi}_q^t, \tilde{\phi}_q^t), (\tilde{\psi}_{u,q}^r, \tilde{\phi}_{u,q}^r)\}$$
$$= \arg\max_{\substack{(\psi_q^t, \phi_{k,q}^t) \in \Theta^t, \\ (\psi_{u,q}^r, \phi_{u,q}^r) \in \Theta^r}} \sum_{u \in \mathcal{U}_q} \sum_{w \in \mathcal{W}_u} \frac{\| \mathbf{h}(f_u^w, d_u) \|^2}{|\eta_L(f_u^w, d_u)|^2}, \quad (6)$$

where $\mathbf{h}(f_u^w, d_u)$ is the effective channel between the AP and user u and with element $h_k(f_u^w, d_u)$ for $k \in \mathcal{K}_q$, Θ^t and Θ^r denote the transmit and receive beamforming codebook, respectively. Denote $\tilde{\mathbf{h}}(f_u^w, d_u)$ as the effective channel of one antenna subarray for user u in group q with analog beamforming angles obtained from (6).

According to the distance-aware multi-carrier transmission strategy, there might be different numbers of users in subcarrier w. Denote the sub-carrier index as w with central frequency f^w and bandwidth B and $\mathcal{W}_u$ as the set of sub-carrier index for user u. Denote $\mathcal{U}^w$ as the set of users sharing the same carrier with central frequency f_u^w with total number U^w. Let q_u be the group index associated with the users $u \in \mathcal{U}^w$. Then, we know that $\mathcal{K}^w = \cup_{u \in \mathcal{U}^w} \mathcal{K}_{q_u}$ represents the set of subarrays transmitting signals in subcarrier w with total number $K^w = \sum_{u \in \mathcal{U}^w} K_{q_u}$.

Let $\mathbf{H}_u = [\mathbf{H}_{1,u}, \mathbf{H}_{2,u}, \ldots, \mathbf{H}_{K^w,u}] \in \mathbb{C}^{M_r N_r \times K^w M_t N_t}$ be the channel matrix for user $u \in \mathcal{U}^w$ with respect to the subarrays in $\mathcal{K}^w$. Then, the effective channel vector $\tilde{\mathbf{h}}_u(f_u^w, d_u) \in \mathbb{C}^{1 \times K^w}$ for user u in group q with analog beamforming is given by

$$\tilde{\mathbf{h}}_u(f_u^w, d_u) = \mathbf{V}_u^H \mathbf{H}_u \mathbf{D}, \quad (7)$$

where $\mathbf{V}_u = \mathbf{a}_r(\tilde{\psi}_{u,q}^r, \tilde{\phi}_{u,q}^r) \in \mathbb{C}^{M_r N_r \times 1}$ represents the receive analog beamforming vector, and $\mathbf{D} \in \mathbb{C}^{K^w M_t N_t \times K^w}$ stands for the transmit analog beamforming operation and is a block matrix with diagonal components given by $[\mathbf{a}_t(\tilde{\psi}_1^t, \tilde{\phi}_1^t), \ldots, \mathbf{a}_t(\tilde{\psi}_{K^w}^t, \tilde{\phi}_{K^w}^t)]$ corresponding to the transmit beam steering vectors for subarrays $k \in \mathcal{K}^w$ and other components all being zero matrix of size $M_t N_t \times 1$.

2) Precoding: We assume that $\tilde{\mathbf{h}}_u(f_u^w, d_u)$ can be perfectly estimated at the user side and fed back to the AP. The equivalent channel matrix for all users can be expressed as

$$\tilde{\mathbf{H}} = [\tilde{\mathbf{h}}_1^T, \ldots, \tilde{\mathbf{h}}_{U^w}^T]^T. \quad (8)$$

Then, maximal ratio transmission (MRT) precoding is given by

$$\mathbf{Q}_{MRT} = \rho_{MRT} \tilde{\mathbf{H}}^{\mathbf{H}}, \quad (9)$$

where $\rho_{MRT} = 1/\sqrt{tr(\tilde{\mathbf{H}}\tilde{\mathbf{H}}^{\mathbf{H}})}$.

Zero-forcing (ZF) precoding is

$$\mathbf{Q}_{ZF} = \rho_{ZF} \tilde{\mathbf{H}}^H (\tilde{\mathbf{H}}\tilde{\mathbf{H}}^H)^{-1}, \quad (10)$$

where $\rho_{ZF} = 1/\sqrt{tr((\tilde{\mathbf{H}}\tilde{\mathbf{H}}^H)^{-1})}$.

3) Quantized Receiver: At user sides, the received vector $\mathbf{r} \in \mathbb{C}^{U^w \times 1}$ is given by

$$\mathbf{r} = \sqrt{P^w}\tilde{\mathbf{H}}\mathbf{Q}\mathbf{s} + \mathbf{n}, \quad (11)$$

where P^w is the transmit power for subcarrier w, $\mathbf{s} \in \mathbb{C}^{U^w \times 1}$ is the Gaussian source data with $\mathbb{E}\{\mathbf{s}\mathbf{s}^H\} = \mathbf{I}_{U^w}$, $\mathbf{Q} \in \mathbb{C}^{K^w \times U^w}$ denotes the linear precoding operation performed at the baseband with $tr\{\mathbf{Q}\mathbf{Q}^H\} = I$. $\tilde{\mathbf{H}} \in \mathbb{C}^{U^w \times K^w}$ is the THz channel with analog beamforming. $\mathbf{n} \in \mathbb{C}^{U^w \times 1}$ is the additive white Gaussian noise (AWGN).

In this paper, we consider the optimal non-uniform ADCs since it provides a tractable and effective way of well characterizing the quantization performance [13]. We will investigate it in the indoor THz communication especially when the size of subarray antennas becomes large.

After the ADC quantization and according to the Bussgang theorem [19], the system output can be written as

$$\mathbf{y} = \mathbf{G}\mathbf{r} + \boldsymbol{\varpi}, \quad (12)$$

where $\boldsymbol{\varpi} \in \mathbb{C}^{U^w \times 1}$ stands for the distortion introduced by the ADCs, and $\mathbf{G} \in \mathbb{C}^{U^w \times U^w}$ is the diagonal matrix modeling the operation of the ADC quantization, which is given by[14]

$$\mathbf{G} = (1 - e_q)\mathbf{I}_{K^w}. \quad (13)$$

and the distortion can be written as

$$\mathbb{E}\{\boldsymbol{\varpi}\boldsymbol{\varpi}^H\} = e_q(1 - e_q)\mathbb{E}\{\text{diag}(\mathbf{r}\mathbf{r}^H)\}. \quad (14)$$

Specifically, considering the case of moderate to high-resolution quantizations, we have the approximation of e_q as [17]

$$e_q \approx \frac{\pi\sqrt{3}}{2} 2^{-2b}. \quad (15)$$

where b specifies the resolution of ADC.

Let $\mathbf{q}_u$ be the u-th column of the precoding matrix $\mathbf{Q}$. Then, the quantized received signal y_u after receiver analog beamforming at user u in group q in subcarrier w can be

described as

$$y_u = \sqrt{P^w}(1-e_q)\tilde{\mathbf{h}}_u(f_u^w, d_u)\mathbf{q}_u s_u + \sqrt{P^w}(1-e_q)\sum_{u'\in\mathcal{U}^w, u'\neq u}\tilde{\mathbf{h}}_u(f_u^w, d_u)\mathbf{q}_{u'}s_{u'} + (1-e_q)n_u + \varpi_u, \quad (16)$$

where $\mathbf{q}_u \in \mathbb{C}^{K^w\times 1}$ denotes the digital precoding vector corresponding to user u, and n_u is the additive white Gaussian noise with power N_0 for user u. ϖ_u is the uth entry of the distortion error $\boldsymbol{\varpi}$.

Then, we know that the achievable rate of user u is lowerbounded by [13]

$$R_u \geq \mathbb{E}\Big[\sum_{w\in\mathcal{W}_u} B\log_2(1+\frac{P^w(1-e_q)^2|\tilde{\mathbf{h}}_u(f_u^w,d_u)\mathbf{q}_u|^2}{\sum_{u\neq u'}P^w(1-e_q)^2|\tilde{\mathbf{h}}_u(f_u^w,d_u)\mathbf{q}_{u'}|^2+\mathbb{E}\{|\varpi_u|^2\}+(1-e_q)^2N_0})\Big], \quad (17)$$

where

$$\begin{aligned}\mathbb{E}\{|\varpi_u|^2\} &= e_q(1-e_q)\mathbb{E}\{diag(\mathbf{r}\mathbf{r}^H)_{u,u}\}\\ &= e_q(1-e_q)\mathbb{E}\{diag((\sqrt{P^w}\tilde{\mathbf{H}}\mathbf{Q}\mathbf{s}+\mathbf{n})(\sqrt{P^w}\tilde{\mathbf{H}}\mathbf{Q}\mathbf{s}+\mathbf{n})^H)_{u,u}\}\\ &= e_q(1-e_q)\mathbb{E}\{P^w\tilde{\mathbf{h}}_u(f_u^w,d_u)(\mathbf{Q}\mathbf{s}\mathbf{s}^H\mathbf{Q}^H)\tilde{\mathbf{h}}_u^H(f_u^w,d_u)+|n_u|^2\} \quad (18)\\ &= e_q(1-e_q)[P^w\sum_{u'}|\tilde{\mathbf{h}}_u(f_u^w,d_u)\mathbf{q}_{u'}|^2+N_0]. \quad (19)\end{aligned}$$

where (18) is derived with $\mathbb{E}\{\mathbf{s}\mathbf{s}^H\}=\mathbf{I}_{U^w}$.

Finally, the sum rate of the indoor THz communication systems is given by

$$R = \sum_{u=1}^{U} R_u. \quad (20)$$

III. Performance Analysis

Based on the discussions in the previous section, we will analyze the achievable rate when the number of subarray antennas goes to infinity.

From [18, proposition 1], the analog beamforming angles of each user group are mainly decided by the AoD/AoA of the LoS path in large subarray antenna regime. Then when the number of subarray antennas goes to infinity, (7) can be rewritten as

$$\tilde{\mathbf{h}}_u(f_u^w,d_u) \xrightarrow{M_t,N_t,M_r,N_r\to\infty} \sqrt{M_tN_tM_rN_r}\Omega_t\Omega_r\mathbf{t}_u(f_u^w,d_u), \quad (21)$$

where

$$\mathbf{t}_u(f_u^w,d_u) = [\mathbf{0}_{1\times\sum_{u'=0}^{u-1}K_{u'}}, \boldsymbol{\eta}_{u,L}(f_u^w,d_u), \mathbf{0}_{1\times\sum_{u'=u+1}^{U^w}K_{u'}}],$$

with $\boldsymbol{\eta}_{u,L}(f_u^w,d_u) = [\eta_{u,1,L}(f_u^w,d_u),\ldots,\eta_{u,K_{q_u},L}(f_u^w,d_u)] \in \mathbb{C}^{1\times K_u}$ denoting the complex gain of the LoS path between user u and subarray $k\in\mathcal{K}_{q_u}$ of the AP in the subcarrier w. K_u represents the number of antenna subarrays allocated to user u. Note that $|\eta_{u,k,L}(f_u^w,d_u)|, k=1,\ldots,K_u$ are the same and denoted as $|\eta_{u,L}(f_u^w,d_u)|$. Obviously, the equivalent channel $\tilde{\mathbf{h}}_u(f_u^w,d_u)$ approaches some determined vector as the number of subarray antennas goes to infinity.

Based on the above analysis, we have the following result on the lower-bound of the achievable rates.

Theorem 1: When the number of subarray antennas approaches infinity, the closed-form lower-bound of the achievable rate of the indoor THz communication system with finite-bit ADCs is given by

$$R^o = \sum_{u=1}^{U} W_u B\log_2\left(1+\frac{1-e_q}{e_q}\right), \quad (22)$$

where $e_q \approx \frac{\pi\sqrt{3}}{2}2^{-2b}$ and W_u is the total number of subcarriers for user u.

Proof: First, we can see from (8), (21), (9) and (10) that

$$\mathbf{Q}_{MRT} = \mathbf{Q}_{ZF} = \frac{1}{\sqrt{\sum_{u\in\mathcal{U}^w}\parallel\boldsymbol{\eta}_{u,L}\parallel^2}}\boldsymbol{\Delta}, \quad (23)$$

where $\boldsymbol{\Delta}$ is

$$\boldsymbol{\Delta} = \begin{bmatrix} \boldsymbol{\eta}_{1,L}^H(f_1^w,d_1) & \mathbf{0}_{K_1\times1} & \cdots & \mathbf{0}_{K_1\times1} \\ \mathbf{0}_{K_2\times1} & \boldsymbol{\eta}_{2,L}^H(f_2^w,d_2) & \cdots & \mathbf{0}_{K_2\times1} \\ \vdots & \vdots & \ddots & \vdots \\ \mathbf{0}_{K_{U^w}\times1} & \mathbf{0}_{K_{U^w}\times1} & \cdots & \boldsymbol{\eta}_{U^w,L}^H(f_{U^w}^w,d_{U^w}) \end{bmatrix}. \quad (24)$$

Then, (19) can be rewritten as

$$E\{|\varpi_u|^2\} = e_q(1-e_q)[P^wM_tN_tM_rN_r\Omega_t^2\Omega_r^2K_u^2|\eta_{u,L}(f_u^w,d_u)|^2+N_0]. \quad (25)$$

Incorporating (17), (23)-(25) and after simple computations, we derive (22) by noting that $\frac{N_0}{M_tN_tM_rN_r}\to 0$. □

Remark 1: It is interesting that the transmission rate with quantized ADCs at user sides is robust to the transmit power and mainly depends on the distortion parameters. Obviously, when b increases, i.e., higher-resolution ADCs, e_q decreases and hence the achievable rate R^o increases.

Remark 2: When the number of subarray antennas goes to infinity, the Gaussian noise can be ignored and the interference source is mainly the quantized distortion. Besides, the interference among user groups is eliminated due to the strategy of allocating different number of subarrays to different user groups and the strong directionality of the large antenna subarray.

Moreover, there may be phase uncertainties for the THz band, which will decrease the achievable rate [10]. Assume that the random phase uncertainties follow uniform distribution in $[-\varepsilon_t(f),\varepsilon_t(f)]$ and $[-\varepsilon_r(f),\varepsilon_r(f)]$ at the transmitter and receivers, respectively. We have the following result.

Proposition 1: In the downlink THz communication system with finite-bit ADCs at user sides, the rate loss caused by the phase uncertainties can be ignored when the number of subarray antennas goes to infinity.

Proof: As proved in [18, Appendix C], the equivalent channel with phase uncertainties can be written as

TABLE I
TRANSMISSION WINDOWS

	Distance	Transmission Windows (THz)	User Group
User1	10m	0.6-0.7, 0.8-0.95	group1
User2	5m	0.6-0.725, 0.8-0.925	group2
User3	1m	0.5-0.6, 0.7-0.8, 0.95-1	group1

TABLE II
SYSTEM PARAMETERS

Parameters	Values
Ω_t, Ω_r	20 dBi, 20 dBi
B	5 GHz
K	8
N_0	-75 dBm
$\varepsilon_t(f), \varepsilon_r(f)$	$\frac{\pi}{18}, \frac{\pi}{18}$

$$\tilde{\mathbf{h}}_u(f_u^w, d_u) \xrightarrow{M_t,N_t,M_r,N_r\to\infty} \sqrt{M_tN_t - (M_tN_t-1)\frac{\varepsilon_t^2(f)}{3} + \frac{\varepsilon_t^2(f)}{3}} \times \sqrt{M_rN_r - (M_rN_r-1)\frac{\varepsilon_r^2(f)}{3} + \frac{\varepsilon_r^2(f)}{3}}\Omega_t\Omega_r\mathbf{t}_u(f_u^w, d_u). \quad (26)$$

Incorporating (26) and (23)-(25), we can also derive the formulation (22) when $M_t, N_t, M_r, N_r \to \infty$. □

***Remark** 3:* This is generally different from the previous study that rate loss will increase as the number of antennas increases. The main reason is that the distortion error caused by coarse quantization dominates the system performance.

IV. NUMERICAL RESULTS

In this section, we evaluate the performance of the indoor THz communication systems with finite-bit ADCs at the receivers. The numerical parameters are given in Tables I and II. In addition, we assume the same size for each subarray, i.e., $M_t = N_t = M_r = N_r$.

Fig. 2 plots the achievable rate with analog beamforming angles selected from the codebook or AoA/AoD of the LoS path for single-user, respectively. From this figure, we can see that the beamforming angle, no matter for one-bit or 3-bit ADCs at the receiver, is decided by the LoS path when the size of the subarray antenna becomes large. Also, we can find that the rate becomes a constant and is independent of the transmit power when the number of subarray antennas goes to infinity as indicated by Theorem 1. Besides, we can find that more transmission power are required to achieve the rate ceiling with higher-resolution ADCs at the receiver. This is generally due to the small distortion component compared with noise in relatively lower transmission power with higher-resolution

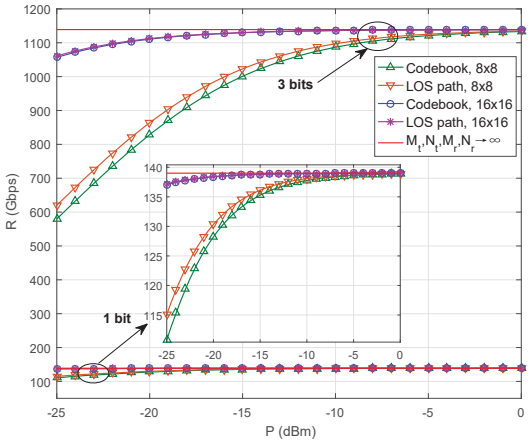

Fig. 2. Comparion of different analog beamforming methods.

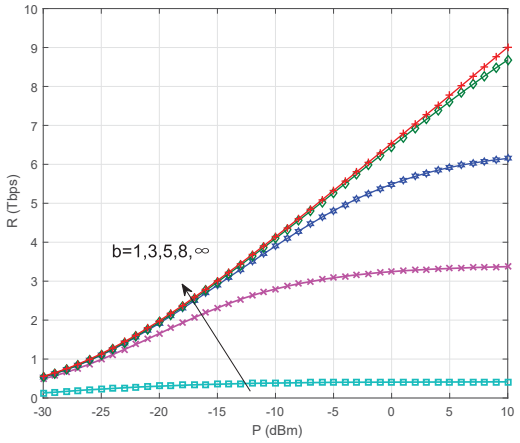

Fig. 3. Achievable rate with finite-bit ADCs.

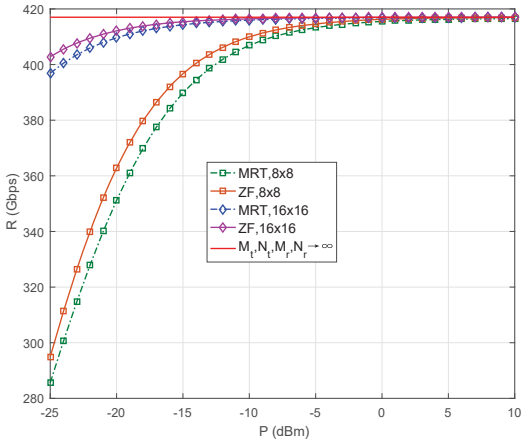

Fig. 4. Comparison of different precodings.

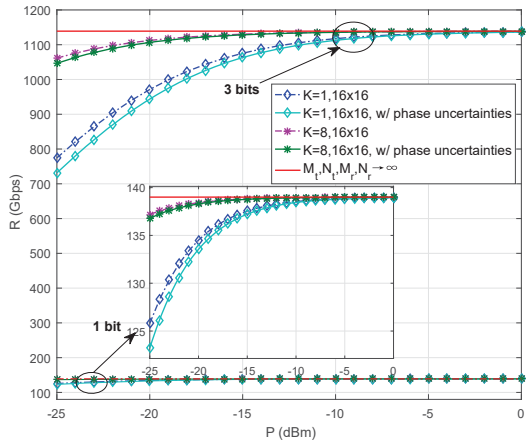

Fig. 5. The effect of phase uncertainties on performance.

ADCs. Subsequently, we assume the analog beamforming angles of each user group are based on the AoD/AoA of the LoS path.

Fig. 3 plots the achievable rate with different resolutions of ADCs. From the figure, we can see that the quantized transmission rate increases as b increases and can achieve almost the same performance as the unquantized transmission rate when $b = 8$, which shows that even the system with finite-bit ADCs can achieve performance close to the infinite-resolution one so that the hardware complexity and cost can be excessively reduced.

Fig. 4 plots the achievable rate with different digital precoding methods in large subarray antennas. Specifically, we randomly allocate 5 antenna subarrays to group 1 and 3 antenna subarrays to group 2. The result shows that the rate uppperbound is consistent no matter for MRT precoding or ZF precoding. We can also see that the interference among users can be ignored when the number of subarray antennas goes to infinity as described in Theorem 1.

Fig. 5 plots the impact of phase uncertainties on the achievable rate with one-bit and 3-bit ADCs for single-user, respectively. From the illustration, we can see that when the number of subarray antennas goes to infinity, the rate loss due to phase uncertainties can be ignored. Also, we can see that the rate loss with multi-bit ADCs at low power is larger than that with one-bit ADCs but can still be negligible when the size of subarray is large enough. We can also find that the phase uncertainties could be reduced when increasing the number of antenna subarrays K for finite subarray antennas. Alternatively, increasing the number of antenna subarrays might won't improve the system performance since the size of the subarray antennas is pretty large.

V. Conclusion

In this paper, we have considered the downlink indoor THz communication system with finite-bit ADCs at user sides. We have assumed the array-of-subarray antenna architecture and distance-aware strategy are employed in the systems. We have derived the closed-form lower bound expression of the transmission rate, which is only related to the distortion factor when the number of the subarray antennas goes to infinity. We have shown that the finite-bit quantized transmission rate can achieve almost the same performance as unquantized transmission rate. In addition, we have proved the achievable rate is robust to the phase uncertainties in large subarray antenna regime. We have also provided numerical results in accordance with our analyzes as well.

References

[1] K. C. Huang and Z. Wang,"Terahertz terabit wireless communication," *IEEE Microw*. Mag., vol. 12, no. 4, pp. 108-116, Jun. 2011

[2] R. Piesiewicz *et al.*, "Short-range ultra-broadband Terahertz communications: concepts and perspectives," *IEEE Antennas Propag. Mag.*, vol. 49, no. 6, pp. 24 - 39, Dec. 2007.

[3] H. Song and T. Nagatsuma, "Present and future of Terahertz communications," *IEEE Trans. Terahertz Science and Tech.*, vol. 1, no. 1, pp. 256-263, Sep. 2011.

[4] I. F. Akyildiz, J. M. Jornet, and C. Han, "Terahertz band: next frontier for wireless communicaions," *Phys. Commun.*, vol. 12, no. 2, pp. 16 - 32, Sep. 2014.

[5] J. M. Jornet and I. F. Akyildiz, "Channel modeling and capacity analysis for electromagnetic wireless nanonetworks in the Terahertz band," *IEEE Trans. Wireless Commun.*, vol. 10, no.10, pp. 3211-3221, Oct. 2011.

[6] S. Priebe and T. Krner, "Stochastic modeling of THz indoor radio channels," *IEEE Trans. Wireless Commun.*, vol. 12, no. 9, pp. 4445-4455, Sep. 2013.

[7] C. Han, A. O. Bicen, and I. F. Akyildiz, "Multi-ray channel modeling and wideband characterization for wireless communications in the Terahertz band," *IEEE Trans. Wireless Commun.*, vol. 14, no. 5, pp. 2402 - 2412, May 2015.

[8] C. Han and I. F. Akyildiz, "Distance-aware bandwidth-adaptive resource allocation for wireless systems in the Terahertz band," *IEEE Trans. Terahertz Science and Tech.*, vol. 6, no. 4, pp. 541 - 553, Jul. 2016.

[9] C. Lin and G. Y. Li, "Adaptive beamforming with resource allocation for distance-aware multi-user indoor terahertz communications," *IEEE Trans. Wireless Comun.*, vol. 63, no. 8, pp. 2985-2995, Aug. 2015.

[10] C. Lin and G. Y. Li, "Indoor Terahertz communications: how many antenna arrays are needed?" *IEEE Trans. Wireless Commun.*, vol. 14, no. 6, pp. 3097-3107, Jun. 2015.

[11] C. Lin and G. Y. Li, "Terahertz communications: an array-of-subarrays solution," *IEEE Commun. Mag.*, vol. 54, no. 12, pp. 124 - 131, Dec. 2016.

[12] M. M. Molu, P. Xiao, M. Khalily, K. Cumanan, L, Zhang, and R, Tafazolli. " Low-complexity and robust hybrid beamforming design for multi-antenna communication systems." *IEEE Trans. Wireless Commun.*, vol. 17, no. 3, pp. 1445-1459, Mar. 2018.

[13] S. Jacobsson, G. Durisi, M. Coldrey, T. Goldstein, C. Studer,"Throughput analysis of massive MIMO uplink with low-resolution ADCs," *IEEE Trans. Wireless Commun.*, vol. 16, no. 6, pp. 4038 - 4051, Jun. 2017.

[14] J. Xu, W. Xu, F. Shi, and H. Zhang, "User loading in downlink multiuser massive MIMO with 1-bit DAC and quantized receiver," in *IEEE VTC* 2017-Fall, Toronto, CA, Sep. 2017.

[15] J. Xu, W. Xu, and F. Gong, "On performance of quantized transceiver in multiuser massive MIMO downlinks," *IEEE Wireless Comun. Lett*, vol. 6, no. 5, Oct. 2017.

[16] C. Molln, J, Choi, E. G. Larsson, and R. W. Heath, "Uplink performance of wideband massive MIMO with one-bit ADCs," *IEEE Trans. Wireless Commun.*, vol. 16, no. 1, pp. 87-100, Jun. 2017.

[17] A. Mezghani and J. A. Nossek, "Capacity lower bound of MIMO channels with output quantization and correlated noise," in *Proc. IEEE. ISIT,* Cambridge, MA, USA, Jul. 2012, pp. 1-5.

[18] D. Li, D. Qiao, L. Zhang, and G. Y. Li, "Performance analysis of indoor THz communications with one-bit precoding" to appear at the IEEE Globecom 2018. Available:http://arxiv.org/abs/1807.00327.

[19] J. J. Bussgang, "Crosscorrelation functions of amplitude-distorted Gaussian signals," Res. Lab. Elec., Cambridge, MA, Tech. Rep. 216, Mar. 1952.